Segmental Dynamics in Homogeneous 1,4-Polyisoprene–1,2-Polybutadiene Diblock Copolymers

J. Kanetakis and G. Fytas*

Foundation for Research and Technology, Hellas (FORTH), P.O. Box 1527, 71110 Heraklion, Crete, Greece

F. Kremer and T. Pakula

Max-Planck-Institut für Polymerforschung, P.O. Box 3148, 6500 Mainz, Germany

Received November 7, 1991; Revised Manuscript Received January 28, 1992

ABSTRACT: The segmental dynamics associated with the primary relaxation process in three homogeneous diblock copolymers of poly(1,4-isoprene-*co*-1,2-butadiene) (PIP–PVE) with similar degree of polymerization N but different composition were investigated by depolarized Rayleigh scattering (DRS) and dielectric (DS) and mechanical (MS) spectroscopy. The entropically mixed samples are well in the disordered phase with $\chi N \sim 0$ (χ being the interaction parameter) and hence exhibit a single glass transition (T_g). For the symmetric PIP–PVE, the first careful DRS experiment and the complementary DS measurements clearly reveal two primary relaxation processes which are not a simple superposition of the relaxation functions of the two components. This dynamic modification is better documented for the asymmetric PIP–PVE reach in PIP which is selectively probed by DRS. For all copolymer samples, the overall shape of the distribution function is virtually temperature independent. The pertinent experimental results are consistent with the "cigar" form of a single diblock copolymer chain in the isotropic melt ($\chi \sim 0$) as suggested by recent Monte Carlo simulations.

Introduction

Bulk copolymers have attracted the interest of polymer scientists in the last 10 years.[1] Most of the work concerns static properties in the disordered and more often in the ordered phase with fascinating microdomain structure. The order–disorder transition is the result of a delicate balance between contradicting thermodynamic forces expressed in the reduced quantity $(\chi N)_s$ (χ being the segment–segment interaction parameter and N the degree of polymerization of the copolymer). Below the microphase-separation temperature T_s, microdomains are formed with maximal composition fluctuations and the length scale is about the copolymer dimension. At temperatures far above T_s, $\chi N \ll (\chi N)_s$ and the amplitude of composition fluctuations in a homogeneous diblock should be small.

The thermodynamically driven concentration fluctuations should also manifest themselves in the local segmental and large-scale chain motions of block copolymers. However, in contrast to the numerous investigations of static properties only a few dynamic studies are known.[2-4] Powerful techniques sensing local motions and covering the necessary broad dynamic range are photon correlation (PCS) and broad-band dielectric (DS) spectroscopy. Moreover, employing PCS in the so-called VH scattering geometry, it is feasible to focus selectively on the dynamics of the more anisotropic block segments. Alternatively, DS is sensitive to segmental motions through the component of the dipole moment perpendicular to the chain contour and can therefore yield valuable complementary information. For polymers possessing a nonzero dipole moment parallel to the chain contour, DS can also measure large-scale (Rouse-like) chain motions.[5]

Block copolymers of 1,4-polybutadiene (PBD) and 1,2-polybutadiene [or poly(vinylethylene) (PVE)] near T_s have shown a two-peak structure for the primary (α-) relaxation in the dielectric loss (ϵ'') spectrum even in rheologically and thermodynamically homogeneous samples.[2] Large-amplitude composition fluctuations even far above T_s were proposed to account for the dielectric behavior. While for microphase-separated samples this explanation is in accordance with the microdomain static structure, in the disordered phase differences in the mobility of chemically dissimilar segments might be an alternative explanation.[4,6] On the other hand, a single broad $\epsilon''(\omega)$ was recently observed on polystyrene (PS)–poly(phenylmethylsiloxane) (PPMS) block copolymer samples rich in PS near and above T_s.[7]

The purpose of this work is to assess the influence of these thermodynamic and kinetic factors on the segmental motion of the block chains. We have chosen the block copolymer *cis*-1,4-polyisoprene (PIP)–1,2-polybutadiene (PVE) at three compositions (75, 50, and 25 wt % PIP) mainly because of its extremely low interaction parameter[8] χ ($<10^{-4}$) and the difference in the optical anisotropy per monomer ($\langle\gamma^2\rangle/x$) of its components; $\langle\gamma^2\rangle/x$ amounts to 11 and 3.5 Å^6 respectively for PIP[9] and PVE. The ϵ''_{max} values of the primary relaxation peaks in bulk PIP and PVE are similar. We have measured the time correlation functions of the fluctuations in optical anisotropy of the undiluted PIP–PVE block copolymers over the broad time range 10^{-5}–10^2 s at different temperatures near and above the single T_g of the samples. Complementary information concerning the α-relaxation in the disordered copolymer was obtained from DS measurements. The combined results rather suggest the manifestation of mobility effects in highly compatible PIP–PVE copolymers which, however, on a local scale should be heterogeneous.

Theoretical Background

Depolarized Rayleigh Scattering. In the molecular theory of light scattering, fluctuations in the anisotropic part $\hat{\alpha}$ of the polarizability tensor give rise to the depolarized component of the scattered light.[10] In the commonly used anisotropic scattering geometry, the incident laser beam propagates in the xy plane with polarization parallel to the z-axis (vertical, V, to the scattering plane xy) and the scattered light is observed in the x direction. For polarization parallel to the y-axis (horizontal H) the time correlation function $S_{VH}(q,t)$ at a scattering vector

0024-9297/92/2225-3484$03.00/0

q measured in a depolarized dynamic light scattering experiment using photon correlation spectroscopy has the form

$$S_{VH}(q,t) = \langle \sum_{i,j} \alpha_{yz}(i,0)\, \alpha_{yz}(j,t)\, \exp\{iq[r_j(t) - r_i(0)]\} \rangle \quad (1)$$

where $\alpha_{yz}(j,t)$ is the yz component of the laboratory-fixed polarizability tensor of the jth segment located at $r_j(t)$ and $\langle ... \rangle$ denotes a statistical average.

For undiluted polymers the segments i and j can belong to the same or different chains and there is no rigorous calculation of the general expression in eq 1. The exponential term reflects the center of mass translational motion, whereas segmental reorientation affects the preexponential term. For block copolymers or blends[11] composed of components with different optical anisotropy, concentration fluctuations, in addition to the orientational dynamics, can modulate the preexponential factor in eq 1. For light scattering q's, the phase term in eq 1 is not very different from unity and the VH intensity $I_{VH} \sim S(q,0)$ being q-independent is proportional to the correlation volume[12]

$$V_c = 2\pi \int_0^\infty \langle 3\cos^2 \theta_{ij}(r) - 1 \rangle r^2\, dr \quad (2)$$

with $\theta_{ij}(r)$ being the angle between vectors i and j located at a distance r. Depolarized Rayleigh scattering can therefore be employed to study also local dynamics.

Dielectric Relaxation. The dispersion in the dielectric susceptibility $\epsilon^*(\omega)$ is given by

$$\epsilon^*(\omega) - \epsilon_\infty = -\Delta\epsilon \int_0^\infty \frac{dc_\mu(t)}{dt} e^{-i\omega t}\, dt \quad (3)$$

where $\Delta\epsilon = \epsilon_0 - \epsilon_\infty$ is the relaxation strength, with ϵ_0 and ϵ_∞ being the low- and high-frequency limiting values of ϵ. The quantity $c_\mu(t)$ is the dipole–dipole autocorrelation function[13]

$$c_\mu(t) = \sum_{ij} \langle \mu_j(t)\, \mu_i(0) \rangle / \sum_{ij} \langle \mu_j(0)\, \mu_i(0) \rangle \quad (4)$$

where $\mu_j(t)$ denotes the elementary dipole moment in the chain at time t. The correlation function $c_{\mu\perp}(t)$ of the dipole moment component perpendicular to the chain contour is sensitive to segmental motion and is a first-order ($l = 1$) orientation correlation function. For the primary relaxation near T_g, the orientation time obtained from $c_{\mu\perp}(t)$ and the second-order ($l = 2$) orientation function $S_{VH}(t)$ (eq 1) is predicted[14] and found to be very similar.[15] For polymer mixtures or diblock copolymers, however, the two orientation correlation functions can weigh differently the segmental orientation of the two blocks, depending on their segmental anisotropies (a_{yz}) and $\mu_\perp$ values.

Composition Fluctuations. For diblock copolymers A–B, the local density $\rho_A(r)$ of A segments defines the order parameter $\psi(r) = \rho_A(r)/\rho - f$ at point r where ρ is the overall (A + B) segment density and $f = N_A/N$ is the fraction of A segments on each chain composed of $N = N_A + N_B$ segments. The composition fluctuations are given by the static structure factor[16,17]

$$S(q) = \langle \psi_q \psi_{-q} \rangle \quad (5)$$

where ψ_q is the Fourier component of $\psi(r)$ and q denotes the magnitude of the wave vector. In the random-phase approximation, the variation of $S(q,T)$ with scattering vector and temperature is given by

$$S(q,T)^{-1} = U(q)/W(q) - 2\chi(T) \quad (6)$$

where $U(q)$ and $W(q)$, being respectively the sum and the determinant of the matrix composed of the correlation functions of two types of ideal polymer chains, are functions of f, N, and $x = q^2R^2$ (R is the radius of gyration of the copolymer). At constant temperature, $S(q,T)$ attains a maximum value at a given x_m. For $f = 0.5$, $x_m = 3.75$, and hence the correlation length of the composition fluctuations is on the order of the molecular size. Increasing N, or the interaction parameter χ, the so-called microphase-separation transition (MST) will occur. The spinodal point, defined by the condition $S(q_m,T_s)^{-1} = 0$, is reached at a given value $(\chi N)_s$. For $f = 0.5$ the mean-field result is $(\chi N)_s = 10.5$, compared to the result $(\chi N)_s = 2$ for a symmetric binary polymer mixture. Considering fluctuation corrections[17] in the mean-field theory of diblock copolymers leads to a larger $(\chi N)_s$ value.

The amplitude of composition fluctuations according to eq 6 depends on the value χN in relation to $(\chi N)_s$. For $(\chi N) \ll (\chi N)_s$ far above T_s composition fluctuations will be negligibly small, implying a spatially completely disordered phase where entropic factors dominate. This condition seems to be fulfilled by the present diblock copolymers for which a very small χ ($<10^{-4}$) has been reported.[8]

Experimental Section

Photon Correlation Spectroscopy (PCS). The correlation functions $G(t)$ of the light scattering intensity at different temperatures near and above the thermodynamic glass transition were measured at a scattering angle $\theta = 90°$. The light source was an argon ion laser (Spectra Physics 2020) operating at 488 nm, single mode, with an average power of 200 mW. The correlation functions were first obtained with a 28-channel log–lin, single-clipped correlator (Malvern K7027) which covers 4.3 decades in time in one run. Since the diblock correlation functions extended in an unusually broad time range, usually two runs with widely different sampling times were employed and the resulting correlation functions were spliced together. During the course of this work, a new ALV-5000 multiple-sampling-time digital correlator was purchased and employed for the PCS measurements. This full correlator uses 31 different sample times in one run, processes the data into 256 channels, covers a time range of 10^{-6}–10^3 s, and is therefore very well suited for photon correlation spectra extending in a very wide time range like the present copolymers. The PCS results reported in this paper were obtained by means of the ALV-5000 digital correlator. PCS measurements were conducted at low temperatures, close to and above T_g. Temperature ranges were −18 to −55 °C for the diblocks, −15 to −5 °C for PVE, and −49 to −59 °C for PIP.

In a homodyne experiment, the desired normalized field correlation function $g(t)$ is related to $G(t)$ by

$$G(q,t) = A(1 + f^*|\alpha g(q,t)|^2) \quad (7)$$

where A is the base line measured at long lag times, f^* is the instrumental factor calculated by a means of a standard, and α is the fraction of the total scattered intensity associated with the density fluctuations. For the ALV-5000 correlator the base line A fluctuates around 1. Correlation functions were obtained in both polarized and depolarized modes, the latter probing the orientational correlation function and yielding an improved signal-to-noise ratio. Figure 1 shows typical depolarized intensity correlation functions for the symmetric diblock at three temperatures.

Dielectric Relaxation Spectroscopy (DS). The real and imaginary components of the complex dielectric permittivity ϵ^* were measured over the frequency range 10–10^6 Hz using a Solartron–Schlumberger frequency analyzer FRA-1260. The sample was kept between two gold-plated stainless steel electrodes and the temperature varied over the range 210–310 K.

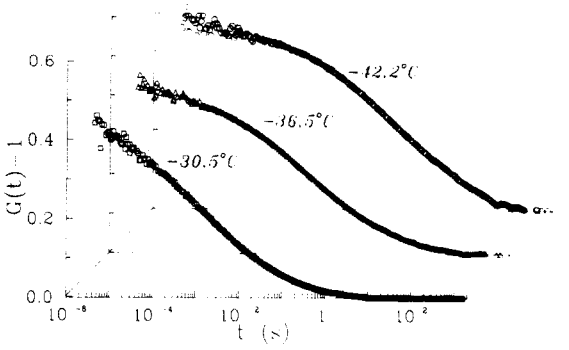

Figure 1. Depolarized intensity correlation functions for PIP–PVE diblock copolymer with PIP fraction $f_{PIP} = 0.43$.

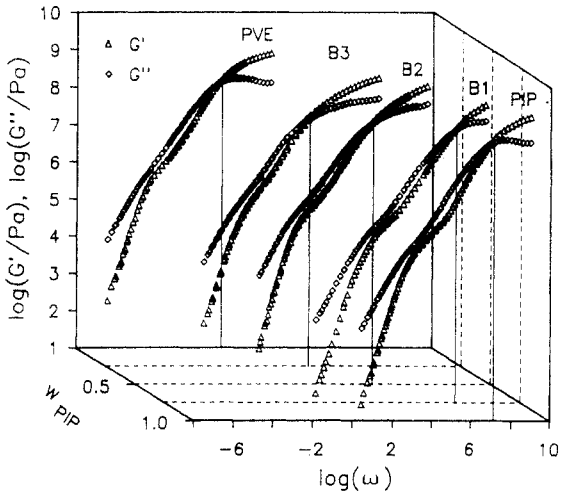

Figure 2. Dynamic shear modulus G' and G'' versus reduced frequency for the three diblock copolymers and the constituent homopolymers.

Table I
Sample Characteristics

sample	structure	$W_{1,4}$[a]	M_w	M_w/M_n	T_g,[b] °C	ΔT_g, K
PIP	1,4 homopolymer	1	2350	1.1	−67	6
B1	1,4–1,2 diblock	0.76	6650	1.04	−64	11
B2	1,4–1,2 diblock	0.49	6410	1.03	−52	17
B3	1,4–1,2 diblock	0.28	6900	1.03	−46	17
PVE	1,2 homopolymer	0	4300	1.05	−26	9

[a] Weight fraction of polyisoprene block. [b] 20 K/min heating rate.

Mechanical Relaxation. The dynamic mechanical experiments have been performed by means of the Rheometrics mechanical spectrometer RMS 800. The dynamic storage modulus (G') and the loss modulus (G'') have been measured isothermally as a function of the angular frequency (ω) (0.1–100 rad s^{-1}) of the sinusoidal shear deformation. Cylindrical samples of diameter 6 mm and thickness 1 mm have been deformed between parallel plates of the same diameter. The measurements were conducted under a nitrogen atmosphere at various temperatures over the range of −70 to +120 °C. The temperature has been controlled with an accuracy of ±0.5 °C. The deformation amplitude was varied within the range 0.01–0.5%, remaining always well within a linear viscoelastic range of the sample as tested by appropriate amplitude sweeps. Master curves of G' and G'' vs ω for the present systems constructed by only a horizontal shift of isothermally measured frequency dependences are shown in Figure 2.

Samples. Three diblock poly(1,4-isoprene-*co*-1,2-butadiene) copolymer samples have been used in this study. The symmetric diblock and the polyisoprene sample are the same as those employed in Fabry–Perot interferometry.[4] Table I summarizes the characteristics of these five samples. The procedure for obtaining dust-free samples suitable for light scattering is reported in ref 4. Low Landau–Placzek intensity ratios have been confirmed for all samples, making them suitable for the PCS measurements indicated also from the large amplitude of $G(t)$ (Figure 1). Table I reports the T_g values as measured by differential scanning calorimetry. A broad T_g range, albeit single valued, has been observed for the symmetric diblock ($\Delta T_g = 17$ K) as compared to PIP ($\Delta T_g = 6$ K) at the same heating rate. Broad transitions have also been observed in miscible blends of PVE and PIP,[8] but the temperature range over which the transition occurs is unusually large when there is an abundance of the higher T_g homopolymer PVE.

Data Analysis and Results

The measured intensity autocorrelation functions $G(t)$ near and above T_g have been treated in the homodyne limit (eq 7). The Kohlrausch–Williams–Watts (KWW) function

$$g^*(t) = b \exp[-(t/\tau)^\beta] + c \tag{8}$$

has been a first attempt to fit the experimental $(G(t)/A - 1)^{1/2}$, treating b, τ, β, and c as adjustable parameters. Parameter c is included in order to account for a nonzero and finite base line observed in some cases. τ is the relaxation time, and the distribution parameter β is a measure of the broadness of the correlation function. In the coupling model,[27] the KWW function results from the retardation of the relaxation due to segmental cooperativity. The simplicity of the KWW function and its acceptable performance in fitting intensity autocorrelation functions have made it widely spread among experimentalists.

For very broad distributions, instead of representing the relaxation function $g(t)$ in terms of one or more KWW functions, the nonexponential shape of the relaxation function is best analyzed in terms of a continuous spectrum $L(\tau)$ which represents the distribution of retardation times τ in analogy to the treatment of mechanical data assuming superposition of exponentials. We use the term retardation spectrum because $g(t)$ is related to the compliance.[18] The unnormalized autocorrelation function $g^*(t)$ (eq 8) is then equivalent to

$$g^*(t) = \int_0^\infty L(\tau)\, e^{-t/\tau}\, d\tau \tag{9}$$

Solving eq 9, i.e. extracting $L(\tau)$ from the experimental $g^*(t)$, is an ill-posed problem. Provencher[19] has developed an algorithm, CONTIN, for inverting integrals of the kind in eq 9 in order to obtain the distribution $L(\tau)$. CONTIN computes a constrained regularization solution subject to a combination of two strategies: (1) incorporation of a priori information and (2) parsimony. A priori knowledge, for example, nonnegativity of $L(\tau)$, is important because it can eliminate a large number of otherwise possible solutions, leading to increased accuracy and resolution. The principle of parsimony dictates that, of all solutions that have not been eliminated by the constraints, choose the simplest one, i.e., the solution that reveals the least amount of detail or information that was not already known or expected. Therefore, the detail that it does have is necessary to fit the data and thus more likely to be real and not an artifact. From eq 9 the amplitude b ($=\alpha f^{*1/2}$; eq 7) of the correlation function (eq 8) is given by

$$b = \int_0^\infty L(\tau)\, d\tau \tag{10}$$

and the mean relaxation time $\langle\tau\rangle$ defined as the area under $g(t)$ is given by

$$\langle\tau\rangle = \int_0^\infty \tau L(\tau)\, d\tau / \int_0^\infty L(\tau)\, d\tau \tag{11}$$

Figure 3 shows typical correlation functions for the two homopolymers and the symmetric copolymer B2 samples.

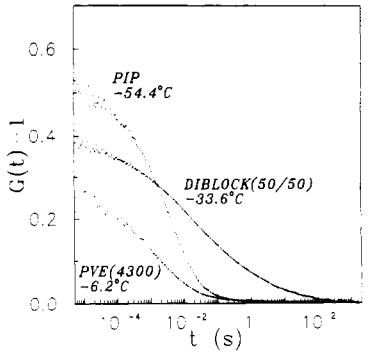

Figure 3. Depolarized intensity correlation functions for PIP–PVE block copolymer with f_{PIP} = 0.43 and the constituent bulk homopolymers PIP and PVE.

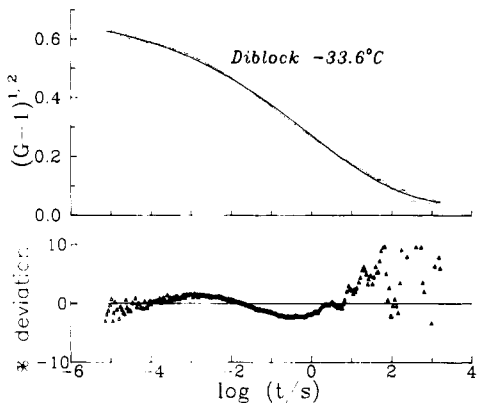

Figure 4. Experimental orientational correlation function for diblock B2 (f_{PIP} = 0.43) and deviation plot for a single KWW fit (eq 8).

The fit of the orientational correlation function $g^*(t)$ to the KWW equation 8 provides the relaxation time τ and the distribution parameter β. β assumes values 0.41 ± 0.03 for PIP, 0.33 ± 0.03 for PVE and 0.22 ± 0.02 for the B2. The disparity between the amplitude of the experimental intensity correlation functions of the two homopolymers is probably due to the presence of a faster β-relaxation ($t < 10^{-6}$ s) in PVE. The remarkably low β value for the diblock B2 as compared to the two homopolymers can be inferred from Figure 3 in which it can be observed that the autocorrelation function of the copolymer covers 8–9 decades in time whereas the respective functions of the homopolymers need only 5–6 decades to relax. Moreover, a KWW fit to the diblock correlation function can only be considered as marginally adequate. Figure 4 depicts the autocorrelation function for the diblock (dots) fitted to a KWW function (eq 8) at -33.6 °C, along with the residuals of the fit expressed as percent deviation. It is apparent that a single KWW function does not present an adequate fit to the experimentally measured correlation functions. There are systematic deviations in the spectra at all temperatures considered. Next we consider employing CONTIN in order to obtain a distribution of retardation times. In order to check its performance[20] for such broad correlation functions, we first used simulated data from a KWW function (eq 8: b = 0.703, τ = 13 320 ms, β = 0.26, c = 0) and performed a CONTIN analysis. Figure 5 shows the correlation function along with the distribution of retardation times for a value of the regularization parameter $a = 4.3 \times 10^{-3}$ which exactly reproduces the intercept b and average time $\langle\tau\rangle$ of the simulated KWW function.

Next we have performed CONTIN analysis of the experimental density autocorrelation functions. Since CONTIN gives a set of solutions with different values of the

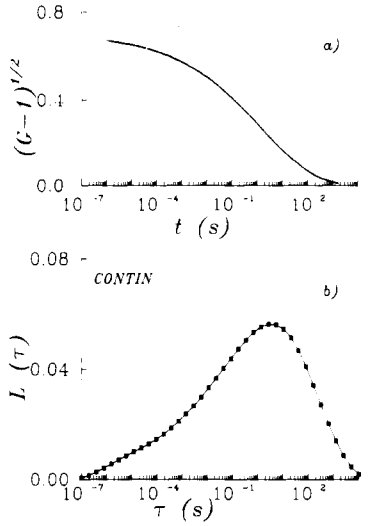

Figure 5. (a) Simulated single KWW function (eq 8; parameters are given in the text) and (b) its distribution of retardation times obtained from eq 9 using the CONTIN algorithm.

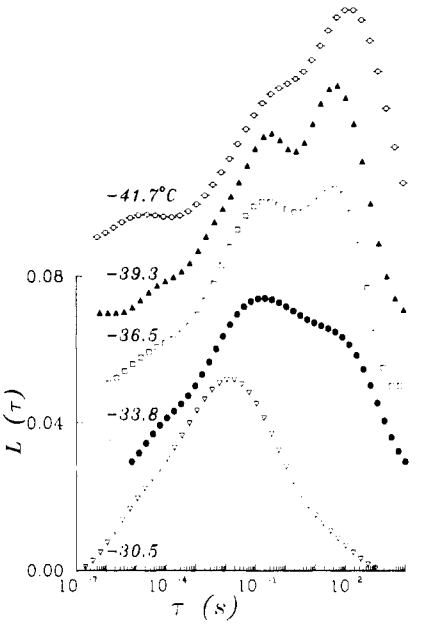

Figure 6. Distribution of orientational times obtained from the inverse Laplace transform (eq 9) of the experimental time correlation functions of B2 (f_{PIP} = 0.43) at different temperatures.

regularization parameter a, we have chosen those with a value equal to or closest to 4.3×10^{-3} corresponding to the simulated data, which in most cases is the CONTIN chosen solution. Figure 6 depicts the resulting distributions of retardation times $L(\tau)$ at five different temperatures. The characteristic feature is not only the broad distribution of relaxation times which is expected in view of the very broad intensity correlation functions but also the dual character of the distribution, evidenced primarily at low temperatures. The two peaks obtained do not have a constant magnitude: the fast peak loses magnitude in favor of the slow peak as temperature decreases toward the glass transition temperature, but both of them contribute to the broad distribution of relaxation times. Parenthetically, we should add that CONTIN gives also solutions with only one peak, but the fits to the orientational correlation functions are characterized by systematic deviations of the residuals. Therefore, one must at least accept that a bimodal distribution of relaxation times as depicted in Figure 6 is a much better representation of the time correlation functions than a unimodal one. The small

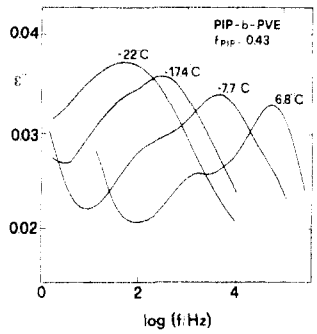

Figure 7. Semilog plot of the dielectric loss (ϵ'') versus frequency for diblock B2 at different temperatures.

shoulders observed in some cases at very fast times result from cutoff effects.

In cases where more than one peak is present, CONTIN allows one to state with more confidence that the data require this number of extrema by imposing the constraint that the solution contains no more than a specified number of extrema. This peak-constrained analysis is performed in a series progressively allowing more extrema with each analysis until a solution is found that is consistent with the data.[19] We have performed peak-constrained analysis to the diblock copolymer data by first imposing the restriction that only one peak is allowed to be revealed. We have found that the solution contains two peaks as before, thus indicating that the presence of the two extrema is not an artifact, but it is indeed the only solution consistent with the data. Needless to say, the peak-constrained analysis by imposing the restriction of two extrema is consistent with CONTIN analysis implemented without this restriction.

It would then be interesting to employ supplementary techniques, other than dynamic light scattering, in order to elucidate the double-peak structure. For this purpose we have employed the DS technique which probes segmental relaxation through $\mu_\perp$, the component of the dipole moment perpendicular to the chain contour. Dielectric spectra were taken over the temperature range −30 to +16 °C. Figure 7 shows curves of ϵ'' versus frequency for various temperatures. These dielectric relaxation spectra depict a similar bimodal behavior with the CONTIN results (Figure 6). There exist two peaks whose relative magnitude changes with temperature. At temperatures far enough from T_g the high-frequency peak has a magnitude exceeding that of the low-frequency peak. As temperature decreases the magnitude of the high-frequency peak increases slightly whereas at the same time the corresponding magnitude of the low-frequency peak increases at a higher rate. At the lowest possible temperature probed by DS, the two extrema have merged into one broad peak. One would consequently anticipate that at even lower temperatures a further increase in the magnitude of the low-frequency peak would have occurred, thus rendering the low-frequency peak of the dielectric relaxation spectra the predominant one. In this low-temperature regime, the PCS results (Figure 6) indeed confirm this expectation; that is, (1) the dual character of the distribution and (2) the dominance of the low-frequency peak over the high frequency one. On the other hand, the mechanical data of Figure 2 support a much broader distribution for the primary relaxation (high-frequency dispersion) in the present diblock copolymers as compared to the homopolymers. By fitting the Fourier transformed KWW function (eq 8) to the frequency dependences of G' and G'' related to the primary relaxation, we obtained $\beta = 0.2$ for the symmetric copolymer B2. Moreover, the observed reasonable time–temperature superposition suggests an overall constant width of the underlying distribution, and the shift factors display experimentally the same temperature dependence with the orientational relaxation times (see Figure 10).

Discussion

Origin of the Distribution. Distribution of relaxation times is a phenomenon observed by several techniques close to T_g. In systems, in which along with free volume effects due to the proximity with T_g we are faced with thermodynamic interactions, the phenomenon becomes more complicated. The symmetric diblock under study provides evidence for a double structure in both DS and PCS measurements. In principle, such a picture implying microscopic heterogeneity could originate from composition fluctuations, mobility effects, or a combination of both. A recent dielectric spectroscopy[2] study has revealed two distinct primary (α) glass–rubber relaxations in nearly symmetric 1,4-polybutadiene (PBD)–poly(vinylethylene) (PVE) diblocks that are considered to be homogeneous ($\chi N \sim 4$) on the scale of SANS, calorimetric, and rheological measurements, and this picture has been attributed to large-amplitude composition fluctuations. Blocks of PIP and PVE are considerably more miscible than the pair PBD–PVE as evidenced[8] by the remarkably low Flory–Huggins interaction parameter ($\chi < 1.7 \times 10^{-4}$) calculated for blends PIP/PVE. Alternatively, two disordered but near to microphase-segregation PS–PPMS diblock copolymers[7] with PS volume fraction 0.82 and 0.89 have shown a broad single $\epsilon''(\omega)$ peak and broad unimodal $L(\ln \tau)$.

According to Leibler's[16] mean-field picture, composition fluctuations (eq 5) are negligible in the disordered, i.e., homogeneous, state. In the fluctuation theory of Fredrickson and Helfand[17] composition fluctuations are important even in the disordered state for finite molecular weights of the blocks and impose qualitative and quantitative changes in the phase diagram and the scattering behavior. The presence of composition fluctuations should broaden the glass transition and hence the distribution of relaxation times deduced from either PCS or DS techniques. The extreme case is the microphase separation in which two distinct peaks are expected and experimentally found.[2,7] It is also known that composition fluctuations are prominent in symmetric diblocks ($f = 0.5$) and become less important as one moves to the composition extrema. Moreover, at constant composition their magnitude increases with the proximity to the MST. One would therefore expect a narrowing of the distribution away from the symmetric composition and from the MST.

Figure 8 shows depolarized intensity correlation functions for the diblocks with PIP fraction 0.23 and 0.71. Typical values of the parameter β of the KWW function (eq 8) are 0.21 ± 0.01 (B3) and 0.37 ± 0.02 (B1). In comparison it should be recalled that, for the symmetric diblock B2, $\beta = 0.22 \pm 0.02$. In addition, the distribution parameters β are found to be insensitive to temperature variations. These experimental findings are supported by the CONTIN analysis. Within the framework of the fluctuation model the distribution of relaxation times for the diblock B3 rich in PVE is unexpectedly broad.

We consider next the dielectric loss curves shown in Figures 7 and 9 for symmetric and asymmetric diblocks, respectively. The diblocks exhibit two distinct α-relaxation peaks, except for the B3 which nonetheless displays a broad peak. The intense peak at low frequencies

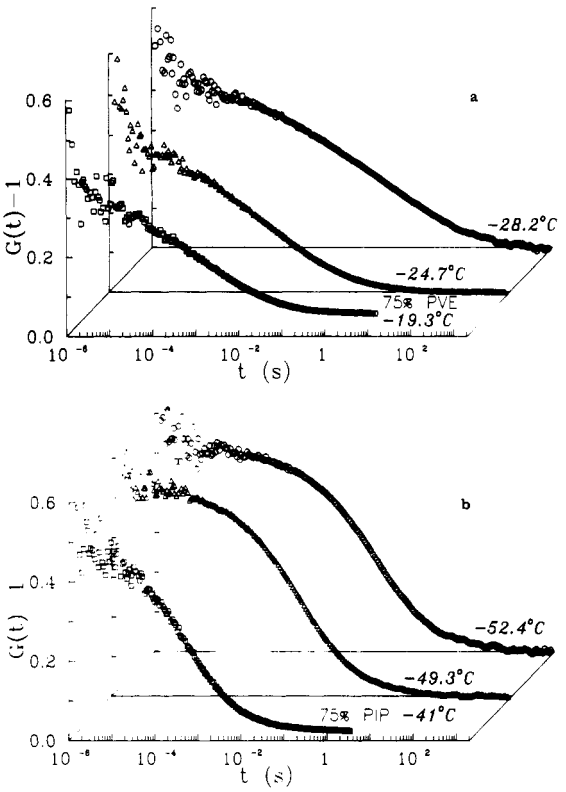

Figure 8. Depolarized intensity correlation functions for the diblock copolymers B3 (a) and B1 (b) respectively with f_{PIP} = 0.23 and f_{PIP} = 0.71 at different temperatures above T_g.

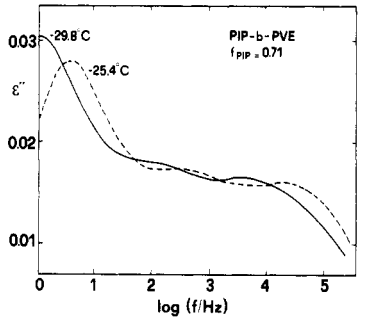

Figure 9. Semilog plot of the dielectric loss versus frequency for the diblock copolymer B1 at two temperatures. The low-frequency peak is due to long-wavelength chain (Rouse-like) motion.

in Figure 9 is due to the normal-model motion of the PIP subchain. The present PIP–PVE diblock copolymers are characterized by $\chi N \sim 0.02$ and hence located far from the MST in the disordered state. It should be recalled that two distinct α-peaks have also been reported[2] in PBD–PVE diblocks which however possess a much larger χN ($\chi N \geq 4$).

In this context, it would be interesting to compare the local dynamic behavior between diblocks and blends consisting of the same components, since it is known that the disordered state of the latter extends over a much restricted region in the phase diagram; at the critical point of the phase diagram $(\chi N)_s^{\text{diblock}} > (\chi N)_s^{\text{blend}}$. We have employed a PIP(5800)/PVE(3200) (numbers in parentheses indicate weight-average molecular weight) monodisperse blend with φ_{PIP} = 0.50 characterized by the interaction parameter at the spinodal point[21] $\chi_s = (1/N_A\Phi_A + 1/N_B\Phi_B)/2 = 0.028$. This blend exhibits larger-amplitude composition fluctuations as compared to the diblocks at the same temperature. The fit of eq 8 to depolarized intensity correlation functions for this blend yields experimentally the same β value with the symmetric diblock, in no apparent relation with the increased magnitude of composition fluctuations at small q's.

From the preceding experimental results, it appears that thermodynamic interactions, inherent in polymer blends and copolymers, alone cannot account for the broad distribution in the homogeneous diblocks with extremely low χN values ($\chi N \to 0$). Moreover, the dual character of the distribution in B1 and B2 implies microscopic (nanometer scale), roughly temperature-independent segregation. This is in accord with the closeness of the results between the diblock B2 and PIP/PVE blend since at large q's their $S(q)$'s are expected to be very similar.

Recent Monte Carlo simulations,[22,23] have shown that a diblock chain in the isotropic melt (χ = 0) assumes a cigarlike form (characteristic for Gaussian chains[24]) with blocks separated along the direction of the end-to-end vector. Such a state can be regarded as a concentration dipole with a correlation length the size of the molecule. For the present copolymers R is estimated to be on the order of 30 Å. The characteristic cooperative length $V_c^{1/3}$ (eq 2) associated with the glass transition is generally accepted[25,26] to involve few monomer units (~10 Å). In view of these concepts the present results reflect demixing in the nanometer range.

Molecular Motions. In a recent ^{13}C NMR[6] study on a miscible PIP/PVE blend, it was found, through the temperature dependence of the line widths, that vinyl carbons on the PVE and PIP segments undergo the transition from the glassy state to the liquid state at different temperatures. It was concluded that, although the blend exhibits a single broad glass transition as seen by DSC, close to T_g different transition rates within a single phase mixture can occur, each of them associated with differing free volume requirements for liquidlike mobility. Thus thermodynamic miscibility does not necessarily imply equivalent glass transition temperatures, in other words, miscible blends can exhibit a "dynamical heterogeneity" notwithstanding their morphological homogeneity. For the blend PIP/PVE, this dynamical heterogeneity is mostly prominent in blends with a high content in PVE. A similar NMR study on diblocks of PIP–PVE has not been performed yet to our knowledge. If, however, we adopt the experimental results of the blend to be valid also in the case of diblocks, then different free volume requirements can evidently result not only in broad relaxation spectra but also in distinct peaks in the relaxation spectrum. The breadth of the glass transition in the entropically miscible PIP/PVE blends is also unrelated to phase segregation effects and thermodynamic miscibility; in fact less miscible blends may exhibit a relatively sharp glass transition. Such anomalously broad glass transitions in certain blends are said to arise not from local concentration fluctuations but from an alteration of the structure of the glass. This interesting phenomenon, however, still needs to be elucidated.

The two homopolymers compared at temperatures equidistant from T_g possess different segmental mobilities and values of the β-parameter. The primary relaxation times for the bulk PIP and PVE obtained from PCS and DS are shown in the Arrhenius plot of Figure 10. The observed agreement between the results of the two techniques was expected in view of recent PCS and DS studies[15] suggesting very close first-order (l = 1) and second-order (l = 2) orientational dynamics near T_g. A Vogel–Fulcher–Hesse–Tamann (VFTH) fit

$$\tau = \tau_0 \exp[B/(T - T_0)] \qquad (12)$$

to the experimental times yields the high-temperature

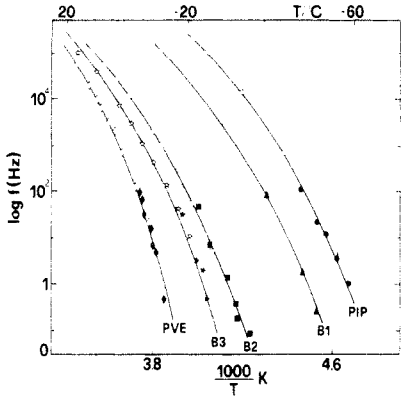

Figure 10. Temperature dependence of the primary relaxation time for three PIP–PVE diblock copolymers and the bulk homopolymers PIP and PVE obtained from photon correlation (solid symbols) and dielectric relaxation (open symbols) spectroscopy. For samples B1 and B2 only the fast relaxation time is shown.

intercept log τ_0 = −12.3 (in seconds), the activation parameter B = 1144K, and the ideal glass transition temperature T_0 = 171 K for PIP and log τ_0 = −12.5, B = 1189K, and T_0 = 215 K for PVE.

The finding that both techniques can resolve two α-relaxation peaks suggests that the correlation volume V_c (eq 2) for segmental reorientation should be at most on the order of the copolymer volume. The appearance of a single glass transition, on the other hand, is probably due to the macroscopical probing length of the DSC. The two characteristic time scales in B2 cannot, however, present the experimental $G(t)$ assuming the distribution parameters (β) of the constituent homopolymers. This is in accord with a recent analysis of the tensile modulus in PIP/PVE blends.[27] This further suggests that the cooperative orientational dynamics of the homopolymers are modified in the copolymer.

Since, as shown before, a single KWW function does not fit the experimental correlation functions adequately, we next have tried a sum of two KWW functions by varying the exponents (β_1, β_2) until a reasonable fit to the experimental correlation function was obtained. The quality of the fit has been checked by the distribution of the residuals. The resulting best fit of the double KWW to the diblock orientational correlation function at T = 33.6 °C with β_1 = 0.32 and β_2 = 0.20 is shown in Figure 11a. The KWW exponents β_1 = 0.32 and β_2 = 0.20 are to be contrasted to the respective values 0.41 for PIP and 0.33 for PVE. This comparison indicates that the components of the diblock lose their characteristic in bulk β values, which now assume much lower values. The phenomenological approach introduced here further shows that by no means is the KWW function for the diblock a superposition of the KWW functions of the two components, nor is the β parameter a simple average of their respective β values; β for both components appears to decrease. In PIP/PVE blends[27] the analysis of the mechanical data using a broadened pair of the KWW functions led to β values falling between those of the homopolymers.

Figure 11b shows the distribution $L(\tau)$ of retardation times obtained by CONTIN employing a sum of two KWW functions with β_1 = 0.32 and β_2 = 0.20, which clearly depicts the dual character of the distribution. The latter is as expected very similar to the $L(\tau)$ of Figure 6 obtained from the CONTIN analysis of the experimental $G(t)$. We have furthermore computed the dynamic loss compliance $D''(\omega)$ to compare with the dielectric $\epsilon''(\omega)$. The former

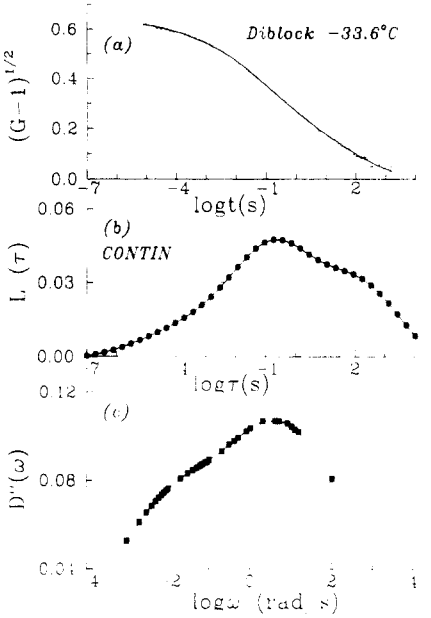

Figure 11. (a) Experimental orientation correlation function for B2 (f_{PIP} = 0.43) block copolymer. (b) Distribution of relaxation times for the double KWW fit to the correlation function of Figure 11a. (c) Dynamic loss compliance from this double KWW function according to eq 13.

was computed via

$$D''(\omega) \propto \omega \int_0^\infty \cos(\omega t)\, g(t)\, dt \qquad (13)$$

where $g(t)$ was analytically given by the double KWW function of Figure 11a. The results of the numerical integration of eq 13, employing the normalized density correlation function $g(t)$, are shown in Figure 11c. The so-obtained $D''(\omega)$ plotted versus frequency exhibits, once more, a bimodal distribution in accord with the results obtained in the time domain (Figure 11b) and $\epsilon''(\omega)$ (Figure 7). It should be emphasized here that, even if the use of two KWW functions has no theoretical basis, the procedure for obtaining $D''(\omega)$ numerically is justified since the sum of two KWW functions is a good representation of the copolymer correlation function $g^*(t)$.

Examination of the $\epsilon''(\omega)$ and $g^*(t)$ data for the two asymmetric diblocks reveals the same interesting similarities and disparities. For the B3 sample rich in PVE, both $L(\tau)$ and $\epsilon''(\omega)$ are single broad peaks characterized by β = 0.21. For the B1 sample rich in PIP, $\epsilon''(\omega)$ clearly displays a two-peak structure in contrast to the single relatively narrow $L(\tau)$ mentioned in the previous section. To account for these experimental findings, we recall that a PVE segment is a weak anisotropic scatterer but has a stronger contribution in the $\epsilon''(\omega)$ as compared to the PIP segment. This useful disparity helps in assigning the relaxation peaks and selectively studying the segmental dynamics of the PIP block. Thus, the short-time peak of the $\epsilon''(\omega)$ spectrum (Figure 9) arises from the PIP-like motion. The latter is modified by the PVE segments as indicated by its reduced β (=0.37) value. It is interesting to notice that this alteration is enhanced in the B3 sample which has a larger PVE content. Thus it appears, in accord with intuition, that the increase of the slower and more cooperative (lower β) component broadens the relaxation distribution function. If the origin of the distribution is the presence of dynamic heterogeneities, then at constant composition a decrease of the temperature toward T_g should augment their influence. However, instead of an overall broadening it is the structure of the $L(\tau)$ (Figure 6) and $\epsilon''(\omega)$ (Figure 7) that varies with decreasing tem-

perature; the slow relaxation process increases its contribution at the expense of the fast mode in B2. At high temperatures far above T_g, free volume effects diminish and fast segmental motion is determined by intrachain conformational transition.[28] Fast segmental dynamics in B2, recently studied by Brillouin scattering,[4] were indeed found to be similar to the faster PIP component.

Concluding Remarks

There is an unambiguous evidence of two primary glass–rubber relaxation processes in diblock copolymers very far ($\chi N \sim 0$) from microphase segregation. The presence of two distinct primary processes in entropically mixed diblock copolymers with different block mobility can be rationalized by involving a cigar shape for the diblock chain. On the basis of the different probing of the block dynamics provided by the presently employed techniques, it appears that the slower PVE dynamics characterized by a larger distribution of relaxation times (smaller β) dominate the copolymer local motions at low temperatures near T_g and impose additional constraints (smaller β) on the PIP segmental dynamics (sample B3).

Acknowledgment. Financial support of the FORTH and Max-Planck-Institut für Polymerforschung is gratefully acknowledged. G.F. thanks Prof. E. W. Fischer for stimulating discussions.

References and Notes

(1) Bates, F. S.; Fredrickson, G. H. *Annu. Rev. Phys. Chem.* **1990**, *41*, 525 and references therein.
(2) Quan, X.; Johnson, G. E.; Anderson, E. W.; Bates, F. S. *Macromolecules* **1989**, *22*, 2451.
(3) Stühn, B.; Rennie, A. R. *Macromolecules* **1989**, *22*, 2460.
(4) Kanetakis, J.; Fytas, G.; Hadjichristidis, N. *Macromolecules* **1991**, *24*, 1806.
(5) See, for example: Yoshida, H.; Watanabe, H.; Adachi, K.; Kotaka, T. *Macromolecules* **1991**, *24*, 2981.
(6) Miller, J. B.; McGrath, K. J.; Roland, C. M.; Trask, C. A.; Garroway, A. N. *Macromolecules* **1990**, *23*, 4543.
(7) Gerharz, B.; Fytas, G.; Fischer, E. W. *Polym. Commun.* **1991**, *32*, 469.
(8) Trask, C. A.; Roland, C. M. *Macromolecules* **1989**, *22*, 256.
(9) Fytas, G.; Floudas, G.; Hadjichristidis, N. *Polym. Commun.* **1988**, *29*, 322.
(10) Zero, K.; Pecora, R. In *Dynamic Light Scattering*; Pecora, R., Ed.; Plenum Press: New York, 1985.
(11) Rizos, A.; Fytas, G., unpublished.
(12) Fischer, E. W.; Strobl, G. R.; Dettenmeier, O.; Stamm, M.; Steidle, N. *Faraday Discuss. Chem. Soc.* **1979**, *68*, 26.
(13) Williams, G.; Watts, D. C.; Dev, S. B.; North, A. M. *Trans. Faraday Soc.* **1971**, *67*, 1323.
(14) Kivelson, D.; Miles, D. *J. Chem. Phys.* **1988**, *88*, 1925.
(15) Boese, D.; Momper, B.; Meier, G.; Kremer, F.; Hagenah, J.-U.; Fischer, E. W. *Macromolecules* **1989**, *22*, 4416.
(16) Leibler, L. *Macromolecules* **1980**, *13*, 1602.
(17) Fredrickson, G. H.; Helfand, E. *J. Chem. Phys.* **1987**, *87*, 697.
(18) Meier, G.; Hagenah, J.-U.; Wang, C. H.; Fytas, G.; Fischer, E. W. *Polymer* **1987**, *28*, 1640.
(19) Provencher, S. W. *Comput. Phys. Commun.* **1982**, *27*, 213; CONTIN (Version 2) Users Manual. Technical Report EMBL-DA07; EMBL: Heidelberg, Mar 1984.
(20) Hagenah, J.-U.; Meier, G.; Fytas, G.; Fischer, E. W. *Polym. J.* **1987**, *19*, 441.
(21) de Gennes, P.-G. *Scaling Concepts in Polymer Physics*; Cornell University Press: Ithaca, NY, 1979.
(22) Fried, H.; Binder, K. *J. Chem. Phys.* **1991**, *94*, 8349.
(23) Pakula, T., submitted for publication in *Macromolecules*.
(24) Pakula, T. *J. Chem. Phys.* **1991**, *95*, 4685.
(25) Donth, E. *J. Non-Cryst. Solids* **1982**, *53*, 325.
(26) Matsuoka, S.; Quan, X. *Macromolecules* **1991**, *24*, 2770.
(27) Roland, C. M.; Ngai, K. L. *Macromolecules* **1991**, *24*, 2261.
(28) Bahar, I.; Erman, B.; Monnerie, L. *Macromolecules* **1991**, *24*, 3618.

Registry No. Poly(1,4-isoprene-*co*-1,2-butadiene) (copolymer), 109264-12-2.